

Analysis of the 2010 Damghan earthquake in Central Alborz (Mw 5.7) and fault-plane identification by H.C method

Fatemeh Armoontan^{1*}, Mehdi Rezapour² and Soheil Azizi³

¹ M.Sc, Institute of Geophysics, University of Tehran, Tehran, Iran

² Professor, Institute of Geophysics, University of Tehran, Tehran, Iran

³ M.Sc, Institute of Geophysics, University of Tehran, Tehran, Iran

(Received: 04 December 2020, Accepted: 01 March 2021)

Abstract

The works done in the study area indicate the potential of the existing fault systems in the region to cause large earthquakes, i.e. magnitude close to 7. In addition, an exact understanding of source parameters gives rise to the recognition of the physical process that occurs as a result of an earthquake. This concept is one of the most important parameters that ultimately leads to the identification of both main and auxiliary planes. The purpose of this study is to determine the mechanism of the Mw 5.7 earthquake occurred in the southeastern region of Damghan at 19:23:48 UTC (23:53:48 local time) on 27 August 2010 (as the biggest event of the last few decades in this region) and its largest aftershock. In this work, nodal planes were first obtained by using time-domain moment tensor inversion method; then, the main fault plane was determined using the geometrical method of H-C which can be implemented by obtaining a centroid moment tensor solution and earthquake focal parameters. Furthermore, the stability of the solution was checked by condition number and jackknifing test. According to the results of this research, a branch of the Toroud fault zone with left-lateral strike-slip motion and northeast-southwest strike was the causative fault of this event. Moreover, the strike, dip and rake of these two events were determined 215, 78, 8 and 222, 66, 11 degrees, respectively. Due to the fact that this area has not been significantly active before, careful monitoring and further studies in such areas is necessary to prevent serious damages.

Keywords: Damghan earthquake, Toroud fault, focal mechanism, waveform inversion, moment tensor inversion

*Corresponding author:

f.armoontan@ut.ac.ir

1 Introduction

Located in the Alpine–Himalayan active mountain belt, the Iranian Plateau is one of the most seismically active regions of the world (Berberian, 2014). A lot number of faults at all over the Plateau and occurrence of frequent earthquakes during the past decades, highlights a need for better estimates of seismic potential in the region (Khodaverdian et al., 2016). The convergence between Arabian and Eurasian plates overcomes the active tectonics of the region (e.g., McKenzie, 1972; Jackson and Mckenzie, 1984; Dewey et al., 1986; Hempton, 1987; Allen et al., 2004; Agard et al., 2011; Mouthereau et al., 2012). Compressional tectonics associated with this continental collision in western Iran forms one of the most quickly deformation and seismically active intercontinental fold-and-thrust belts on the Earth (Talebian and Jackson, 2004; Nissen et al., 2011). High topography, young volcanoes and active faults in the Iranian Plateau cause destructive earthquakes with different mechanisms. The seismicity pattern of Iran shows a high number of earthquakes of medium magnitude and rarely destructive earthquakes with magnitude greater than 6.0 (Norouzi and Hashemi, 2016). Focal mechanisms of earthquakes are important for studying seismotectonics of a region and understanding the physical processes applied to a fault during the occurrence of an event. Furthermore, they serve as a basic input for seismic hazard assessment (Vackar et al., 2017). Although important information such as event location and resolution of focal plane can be extracted from the first few seconds of seismic waveforms, to study in detail, the whole waveform should be used. This type of study can express the focal depth and seismic moment more exactly and provide valuable information on deformation in the area. Waveform modeling is a powerful tool available to

seismologists to correct structural models of the earth and to understand fault rupture processes. In general, waveform modeling is an iterative process (not for point sources) that minimizes the difference between observed and synthetic seismograms by fitting the Earth's structure (Lay and Wallace, 1995). Various methods have been developed to invert waveforms to study the temporal and spatial details of the rupture process and the resulting slip distribution. Owing to the increasing amount of data on a global, regional and local scale, as well as good access to data retrieval, modeling methods are constantly being updated. Based on the available regional data, iterative disconsolation inversion is performed for the all over waveform. The moment tensor is calculated by the least-square minimization of the difference between observed and synthetic data. For creating synthetic waveforms, the full Green's functions (Bouchon, 1981, 2003) are computed, and the spatio-temporal grid search, progressively closer to the true source position and time, is performed. Finally, the fault plane will be determined using the geometric method (H-C method) (Zahradnik et al., 2008) and the seismicity of the area will be mentioned. H-C method is one of several approaches that can distinguish the fault plane from the auxiliary plane. Assuming a planar fault, H-C method works in favorable conditions such as: (1) a reasonably accurate determination of the hypocenter (H) and centroid (C) positions, (2) a sufficient distance between H and C, larger than the uncertainties of the H and C positions, and (3) earthquake geometry that should not be very complex.

Located in 34.25° to 37.33° N latitude and 51.83° to 57.5° E longitude, the study area including Semnan state, is a transition region of three seismic provinces (Fig. 1), and its seismic behavior shows variety. Furthermore,

statistical analysis of historical earthquakes (Ambraseys and Melville, 1982) and instrumental earthquakes (1900-2017) shows that some faults in this region are capable of generating earthquakes with magnitude close to 7.0. The large number of micro-earthquakes in some areas of Semnan indicates the accumulation of stress and energy release. In general, the region is tectonically active and requires further studies as a result. This region is mainly located in the two seismotectonic provinces of Alborz-Azarbayejan in its northern and western parts and Central-Eastern Iran in its southern and eastern parts. It seems that due to the action of parallel faults between these two different regions, geological developments have created a different form of seismicity in Semnan province; therefore, we see different seismic behaviors in two parts of the province. For example, abundance of active faults and earthquakes in the

northern and western parts of Semnan can be easily identified while in the southern and eastern parts, the number of events has greatly decreased. Most faults in this province have a reverse or thrust mechanism (Fig. 1). Destructive events have occurred in the past in Semnan. The most important historical event, the Koumes earthquake, with a magnitude of 7.9 on the surface wave scale, occurred in 856 AD. This event is known as the largest intercontinental earthquake in Iran, and Ambraseys and Melville (1982) described it as a catastrophic earthquake with 200,000 deaths. Fig. 1 shows the epicentral distribution of occurred events in the region with magnitude greater than 4.0 including earthquakes of the historical period up to 2017. As can be seen in this figure, the 2010 Mw 5.7 Damghan earthquake is the most important event in Semnan region, so this event will be reviewed.

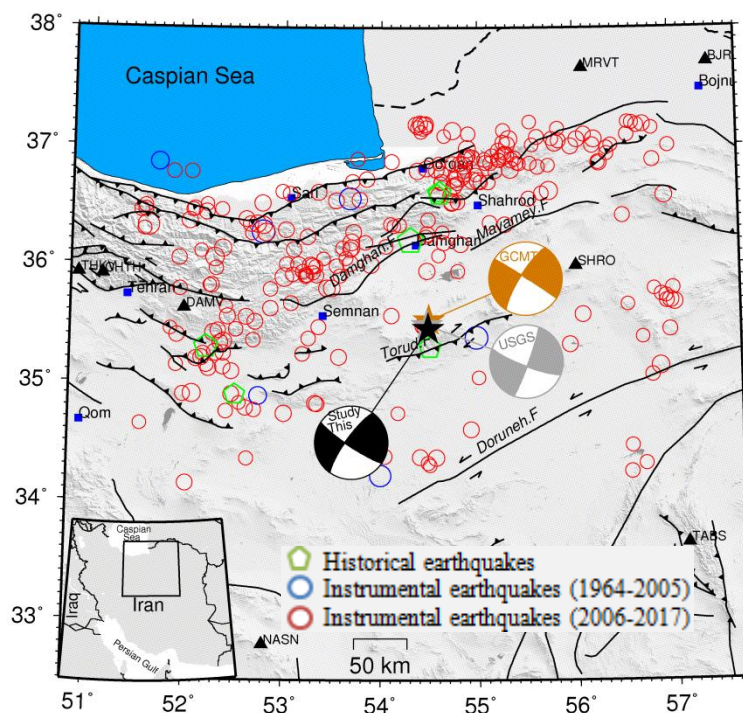


Figure 1. Seismicity map and focal mechanism solutions for Damghan 2010 earthquake reported by GCMT, USGS and this study. Earthquake epicenters with $M > 4.0$ were extracted from the bulletin of the International Seismological Center (ISC) from 1964 to 2005 and from the Institute of Geophysics, University of Tehran (IGUT) for the 2006-2017 earthquakes. The solid lines show traces of major active faults (mapped by Hessami et al., 2003) in the region. Inset is location of the study area on the Iran map.

2 Methodology

Precise knowledge of seismic source parameters is a prerequisite for understanding physical processes on faults during earthquakes. For detailed studies, all seismograms should be considered. These kinds of studies that can impose further constraints on the hypocentral depth and earthquake moment, provide valuable information on deformation style of the region. Complexity of regional and local studies, compared to the teleseismic ones, is obvious at distances of the order of 10–10³ km, where signals are not solely composed of a few simple phases, and due to the abundant of high frequencies, the near-field effects can be significant. Seismic ray theory which is analogous to optical ray theory, is a high-frequency approximation and has several important limitations (Shearer, 2009), so at teleseismic distances, it has to be replaced by full-wave methods representing complete wave fields. Several frequency–wavenumber methods can be used, such as the discrete wavenumber method (Bouchon, 1981) and ISOLated Asperities software package (ISOLA) (Sokos and Zahradnik, 2008) which allows inversion of complete regional and local waveforms for both point source and its spatial and temporal variations (Kikuchi and Kanamori, 1991). The moment tensor is retrieved through a least squares inversion, whereas the position and origin time of point sources are grid-searched. The computation options include inversion to retrieve the full moment tensor (MT), deviatoric MT and pure double couple MT. This assessment combines the signal-to-noise ratio in frequency range of the inversion, waveform fit (hence variance reduction), condition number, and also the space–

time variability of the solution (Sokos and Zahradnik, 2013).

For assessing the double couple percentage (DC%), Zahradnik et al. (2008) suggested complementing the standard least square moment tensor retrieval with a hierarchic spatio-temporal grid search. Getting progressively closer to the likely source position, convergence of the DC% is identified

To identify the causative fault plane, we used the H-C method (Zahradnik et al., 2008). This method is a simple and new method that can be implemented quickly if the solution of the moment tensor and the hypocenter are available. In seismic location methods, based on the time course of seismic waves, the location of the rupture or the so-called hypocenter is determined. Therefore, this place is considered the starting point of the fracture (H). However, the CMT solution obtained by modeling long period wavelengths is the approximation of the point at which the most slip occurs on the fault surface (C). In the CMT solution, according to the determination of the moment tensor elements for the case of double couple, the values of the dip, strike and rake parameters of the two main and auxiliary planes passing through C can be determined; the fault plane will be a plane containing the fracture starting point (H) and point C.

3 Database

Here, the data recorded in the broadband stations of the International Institute of Earthquake Engineering and Seismology (IIEES) with suitable station coverage was used for waveform inversion. The coordinates of these stations are listed in Table 1 and their locations are shown in Fig. 1.

Table 1. Coordinates of IIEES stations.

No.	Station	Latitude(°)	Longitude(°)	Altitude (m)
1	BJRD	37.7	57.408	1337
2	CHTH	35.908	51.126	2250
3	DAMV	35.63	51.971	2300
4	MRVT	37.659	56.089	870
5	NASN	32.799	52.808	2800
6	SHRO	35.99	56.01	1264
7	TABS	33.649	57.119	1106
8	THKV	35.916	50.879	1795

To improve the results, different velocity models were used to calculate the Green's functions. By comparing the results, the most compatible model with the region, i.e. the velocity model of Nemati et al. (2012) was selected for final processing.

To investigate the focal mechanism of the 27 August 2010 earthquake and its largest aftershock, these earthquakes were relocated using the Hypocenter

program (Lienert et al., 1986; Lienert and Havskov, 1995) and the velocity model of Nemati et al. (2012). Table 2 contains information about these events reported by different agencies and this study. It should be noted that in this table, IGUT/IRSC (Institute of Geophysics, University of Tehran) reports hypocenter but GCMT (Global Centroid Moment Tensor) determines the centroid.

Table 2. Location and source parameters of the 2010 Mw 5.7 Damghan earthquake and its largest aftershock as reported by various agencies and this study.

Date	Agency*	Origin time (UTC)	Lat.(°)	Long.(°)	Depth(Km)	Mag.	Strike, Dip, rake (1)	Strike, Dip, rake (2)
2010.08.27	IGUT/IRSC	19:23:49.5	35.488	54.466	6.7	$M_N=5.9$	-	-
	USGS	19:23:49	35.490	54.470	7	$M_w=5.8$	20,85,-10	111,80,-175
	GCMT	19:23:52.4	35.53	54.49	14.9	$M_w=5.8$	212,78,-2	302,88,-168
	IIEES	19:23:48	35.46	54.485	14.1	$M_L=5.9$	-	-
	This study	19:23:48	35.457	54.482	11.5	$M_w=5.7$	124,82,168	215,78,8
2010.08.28	IGUT/IRSC	00:29:05.3	35.485	54.437	6.1	$M_N=5.0$	-	-
	USGS	00:29:05	35.490	54.440	6.0	$m_b=4.9$	-	-
	GCMT	-	-	-	-	-	-	-
	IIEES	00:29:3.2	35.465	54.473	15	$M_L=5.2$	-	-
	This study	00:29:06.04	35.477	54.465	12.5	$M_w=4.7$	222,66,11	127,80,155

*IGUT/IRSC: Institute of Geophysics, University of Tehran; USGS: U.S. Geological Survey; GCMT: Global Centroid Moment Tensor; IIEES: International Institute of Earthquake Engineering and Seismology.

4 Data processing

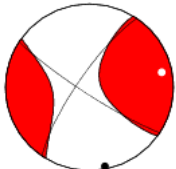
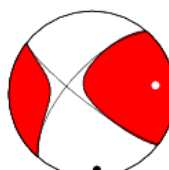
The initial information obtained from the inversion of the waveforms using the waveform recorded at the stations for the main earthquake and the largest

aftershock is given in Table 3. The second column of Table 3 shows the frequency range used in inversion. The best frequency range is selected based on the best variance reduction (maximum

value close to one) for different components of each station. The inversion is performed several times for an event by selecting different frequency intervals and selecting the frequency interval that results in the best response (maximum variance reduction). In the first step, inversion is performed to determine the optimal depth below the reported initial epicenter. The third and fourth columns show the angles of strike, dip and rake obtained for the two

main and auxiliary planes of the focal mechanism. The fifth column shows the optimal depth of the obtained focal depth. The magnitude of the optimized torque, the percentage of two pairs of moment tensor forces and the amount of variance reduction obtained after the initial inversion are listed in columns 6, 7 and 9, respectively. Finally, the last column shows the shape of the focal mechanism for each event.

Table 3. Information obtained from the initial inversion of the seismic moment tensor by ISOLA software.

Date and Time	Frequency (Hz)	Str1, Dip1, Rak1 (°)	Str2, Dip2, Rak2 (°)	Centroid Depth (Km)	Mw	DC%	CN	Var. Red. %	Foc. Mech.
2010.08.27 19:23:48.00	0.02-0.06	124, 82, 168	215, 78, 8	10	5.7	65.7	3.3	80	
2010.08.28 00:29:06.04	0.02-0.06	222, 66, 11	127, 80, 155	8	4.7	82.3	3.0	81	

Using ISOLA package and H-C geometric method and also by modeling the local and regional waveforms, the causative fault of earthquake 27 August 2010, Mw 5.7, is identified. Applying local and regional data allows us to get more details from modeling. In this method, it is tried to determine the fault plane by precisely determining the position of the focal point (H) and the centroid point (C).

The optimal source position and time are grid-searched in three stages (Zahradnik et al., 2008). First, we start with a 20 point grid below the epicenter, at a distance of 1 km from each other.

Based on the preliminary tests, better results are obtained at the depths of 7 to 9 km. Fig. 5-a shows very large double couple percentage changes, from 0 to 100%. At each depth, the moment tensor orientation (strike, dip and rake) corresponding to the optimal time is highly variable with the trial spatial positions, except at about 11 km southeast from the epicenter, where the correlation has its maximum value.

Second, we compute the moment tensors along a vertical line passing through the optimal position from the previous stage, spanning the depths of 9, 10 and 11 km (Figs. 2 and 3). The double

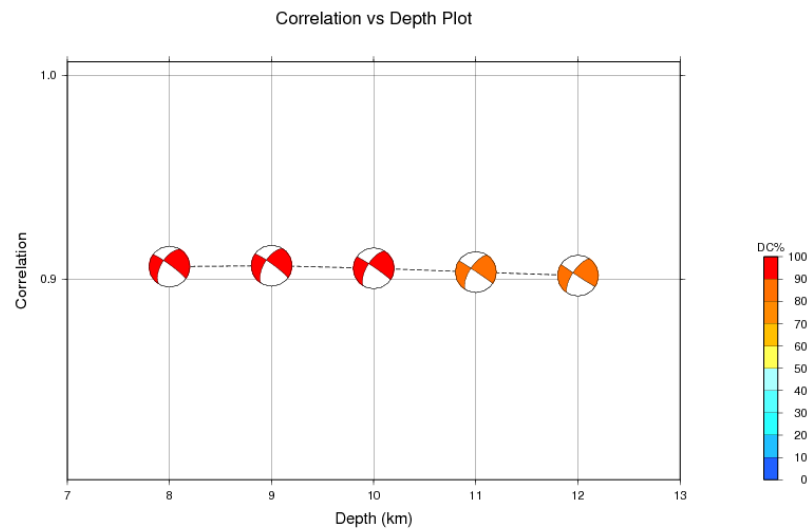


Figure 2. Percentage of depth correlation for frequency ranges of 0.02-0.06 Hz using the velocity model of Nemati et al. (2012). At depths of 8 to 10 km, the highest correlation is observed.

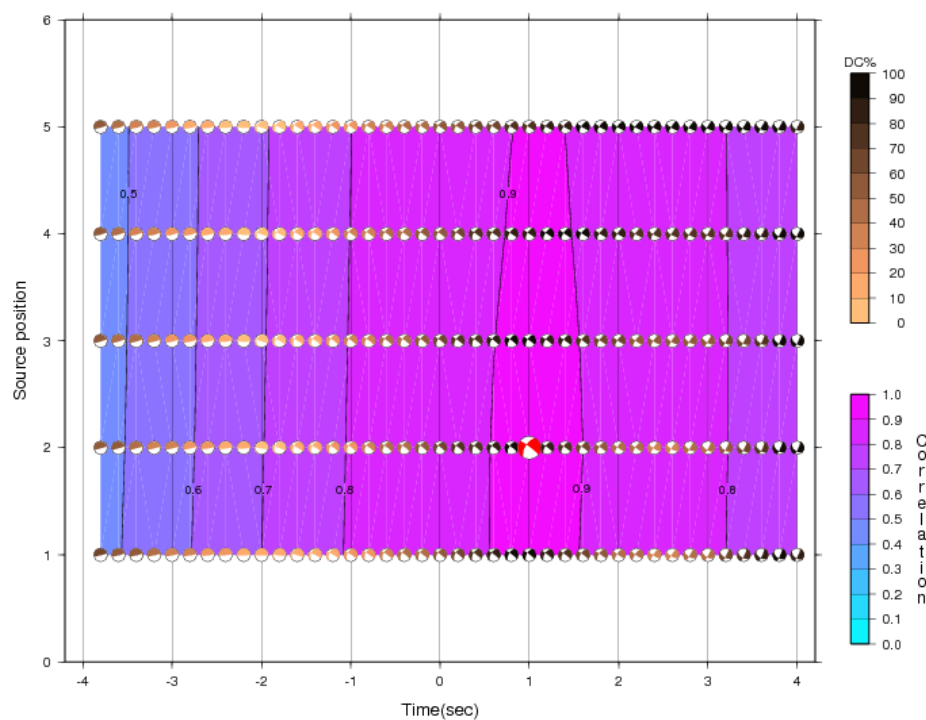


Figure 3. Location of sources at 5 different depths in terms of time shift, correlation and percentage of double couple for the earthquake on 27 August 2010 at 19:23:48.

couple percentage still varies for these three depths from 32 to 90% (Fig. 5-b).

Third, fixing the optimal depth of 10 km, we focus the location and time search to 49 trial positions between the positions. The optimal location is 6.32 km south-east of the epicenter (Fig. 4). The double couple percentage varies for this depth from 60 to 70% (Fig. 5-c). To

investigate the percentage of double couple, the percentage diagram of double couple is drawn in terms of correlation for all three stages of inversion (Fig. 5). Actually, at grid search, the centroid time is estimated in the time range of -4 to $+4$ seconds. In fact, DC% is a function of optimal temporal and spatial positions, which time position has a great impact on

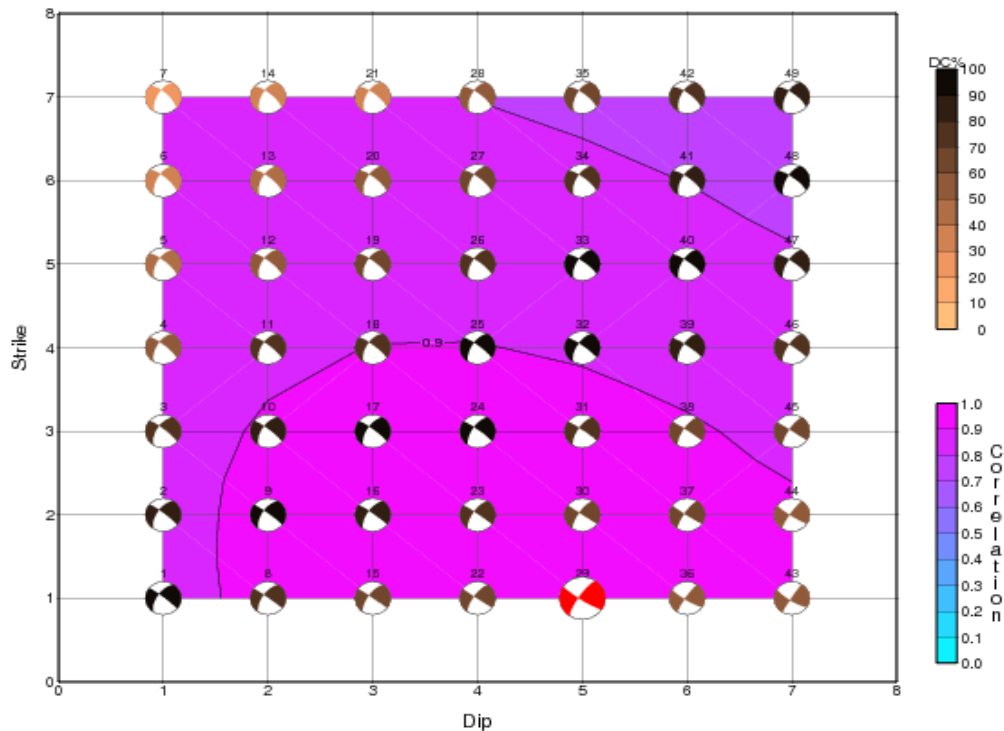


Figure 4. The optimal location of CMT at a depth of 10 km in the third stage of network search. The network consists of 49 points with distances of 2 km from each other based on the degree of correlation and the percentage of double couple.

determining it. In all stages of inversion, the frequency range of 0.02-0.06 Hz was used. As shown in Fig. 5, the red and blue symbols are the optimal temporal and spatial positions of each point element, respectively. In Fig. 5-c, there is strong variation of the DC% with optimal correlation and the red symbols mark the range from 60% to 100%. Table 3 shows the DC% value of 65.7 which is in this range.

Fig. 6 displays the degree of matching of observed and synthetic waveforms. As illustrated in the figure, the observed and synthetic waveforms are in good agreement for most of the station components, because a small number of waveforms that were less compatible and did not show good inversion were removed. The final output of the solution can be seen in Table 3.

The condition number (CN) measures the reliability of the inversion from the perspective of the source-station location,

frequency range and crustal model used. CN does not depend on the particular data used in each inversion; that is, CN can be calculated without using actual waveforms (Zahradnik and Custodio, 2012). Very large (CN>10) or very small values (CN<10) of CN indicates ill- and well-conditioned problems, respectively (Sokos and Zahradnik, 2013) (Table 3). Stability of the solution is checked by a jackknifing test; we repeatedly remove one station and recalculate the inversion (Fig. 8).

Using the same procedure as for the main shock, the largest aftershock, 28 August 2010, Mw 4.7, was studied. For this aftershock, the focal mechanism and the centroid location were determined in three stages. Fig. 7 shows the degree of matching of observed and synthetic waveforms. The final output of this process is shown in Table 3. This aftershock is located about 3 kilometers from the main event.

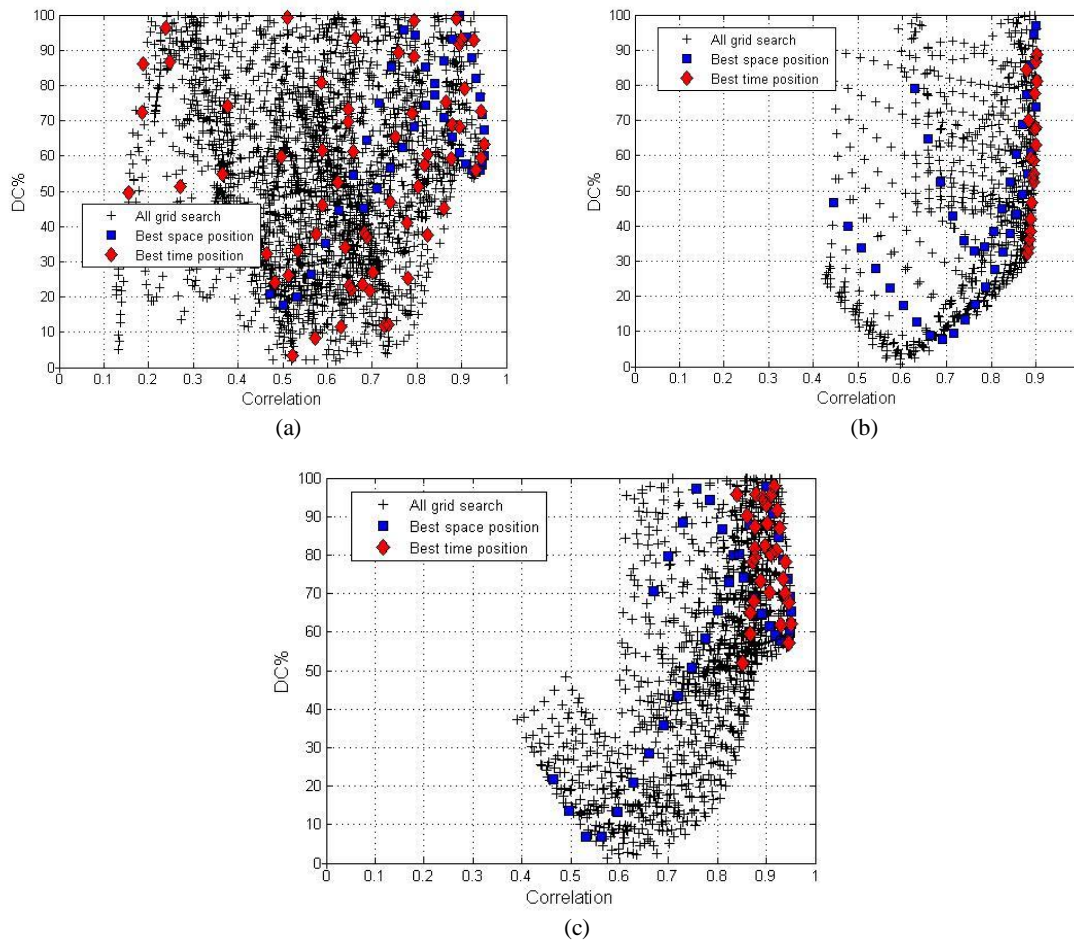


Figure 5. The DC% versus correlation for (a) first stage network search (b) second stage network search (intermediate search) (c) third stage network search. Each plus sign (+) corresponds to a moment tensor calculated in the search network. The red symbols corresponding to the solution of all tests source situations are at the optimal time. Blue symbols indicate changes in the percentage of DC in test times but in the optimal location. Convergence of DC of forces (red symbols) is achieved during steps (a) to (c).

5 Determining the main fault plane with H-C method

The focal mechanism obtained for the main shock (on 27 August 2010, Mw 5.7) which occurred near the Toroud fault is of the left-lateral strike-slip type with a relatively steep dip to the southwest. According to the mechanism of this event and the behavior of the surrounding faults, the causative fault can be introduced as a branch of Toroud fault zone, along the northeast-southwest in the northern part of Toroud fault. Because the location of points H and C is on the main fault plane, a plane with a strike 215° and dip 78° is the main fault plane (Fig. 9). The distance between H

and C is 3.75 kilometers and the direction of rupture is in the north-east.

The focal mechanism of the largest aftershock is a left-lateral strike-slip with a relatively steep dip to the south. It occurred near the Toroud fault. A plane with a strike 222° and dip 66° is the main fault plane (Fig. 9). The distance between H and C, which are on the main fault plane, is estimated 5.76 kilometers and the direction of rupture is in the southwest.

6 Discussion and Conclusion

The earthquake of 27 August 2010, Mw 5.7 and its largest aftershock, $m_b=4.9$, in the southeast of Damghan, are the biggest

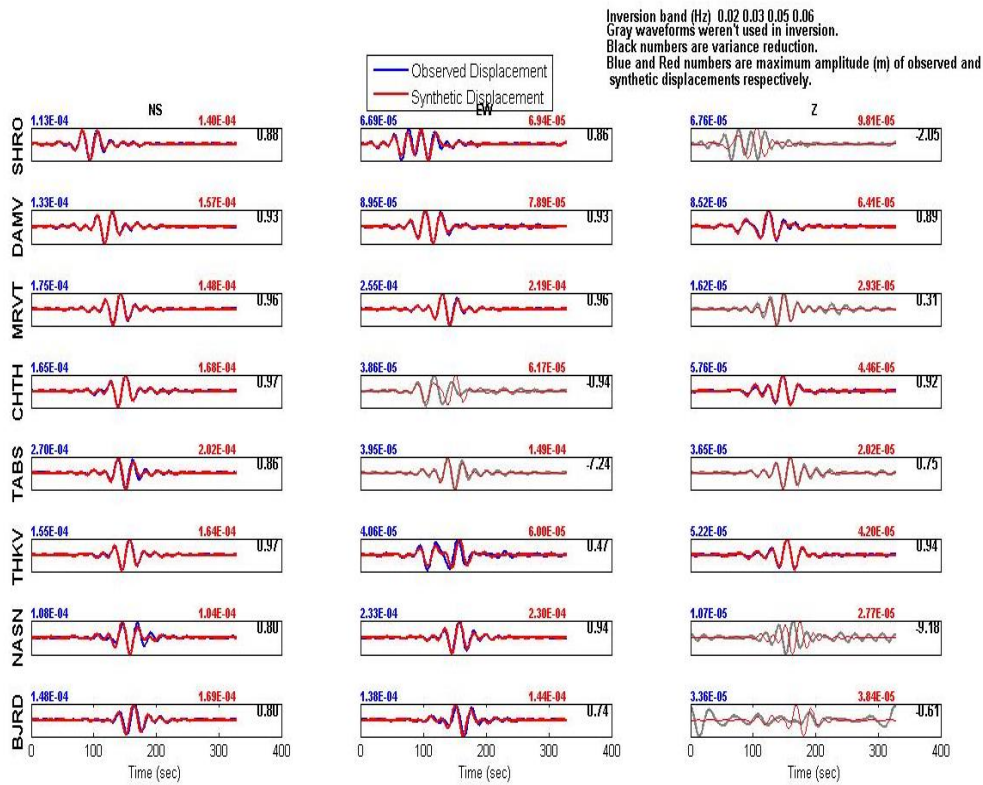


Figure 6. Comparison of observed and synthetic waveforms at different stations for the earthquake on 27 August 2010 at 19:23:48. The blue number at the top of each station component indicates the variance reduction. The components shown in gray have been removed in inversion.

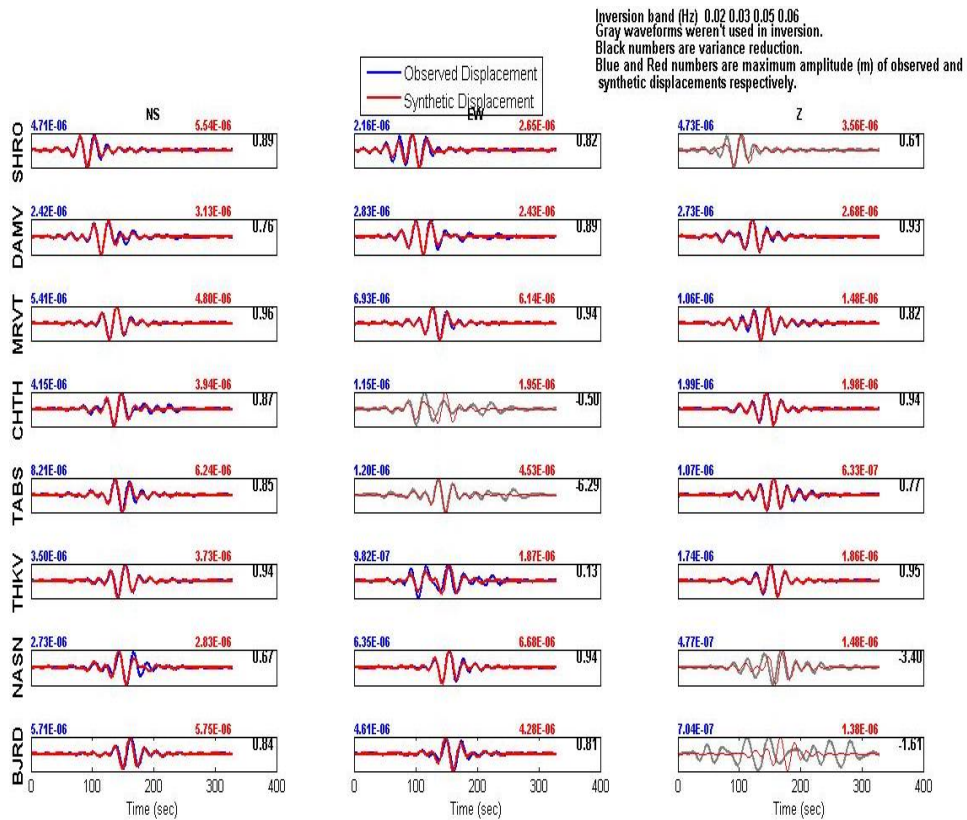


Figure 7. Comparison of observed and synthetic waveforms at different stations for the earthquake on 28 August 2010. The blue number at the top of each station component indicates the variance reduction. The components shown in gray have been removed in inversion.



Figure 8. Test of stability of the focal mechanism of the main shock (left) and its largest aftershock (right) by repeatedly remove of stations (jackknifing). For each removal, a complete space–time grid search and least-squares MT calculations was done. As seen on the nodal planes, the responses are stable.

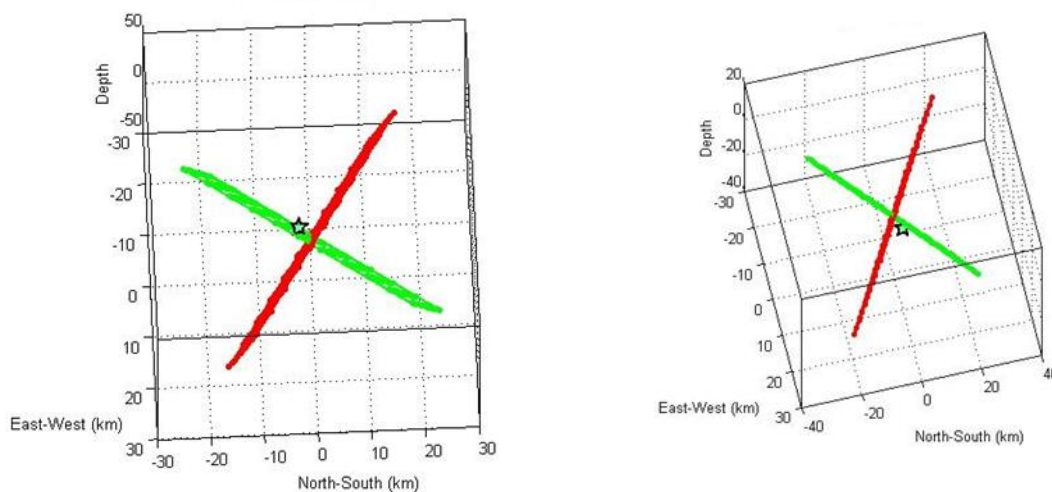


Figure 9. (left) Display a plane with a strike 215 and dip 78 (green screen) as the main fault. The distance from this plane to the hypocenter is estimated at 0.78 km. (right) Display a plane with a strike 222 and dip 66 (green screen) as the main fault. The distance from this plane to the hypocenter is estimated to be 1.35 km. The dip in this figure is less than the dip of the main event. The intersection of the two planes shows the point C and the star is hypocenter point.

recent events in this region. The focal mechanism and the main fault plane were investigated by H-C method for these two events and the mechanism of left-lateral with a steep dip to the southwest was determined. The obtained strike, dip and rake of these two events were 215, 78, 8 and 222, 66, 11 degrees, respectively. A good agreement between results of this research and reports of the seismological centers is seen (Table 2). The causative fault of this event and its aftershock is near Toroud fault. According to the mechanism of this event and the behavior of the surrounding faults, the causative

fault can be a branch of Toroud fault zone, along the northeast-southwest in the northern part introduced the Toroud fault.

Considering the seismic behavior of the region and also having the potential for occurrence of medium and large scale earthquakes, in order to reduce damage, seismicity studies, hazard analysis and accurate knowledge of seismic sources in this region are essential. It seems that the earthquake is related to a branch of Toroud fault that has not had significant activity before, so more detailed monitoring and studies in such areas are

necessary to prevent serious damage. Moreover, due to being in transition region of three seismotectonic states and the diversity of seismic behavior, Semnan is prone to become a small scale laboratory with suitable azimuth coverage.

Acknowledgments

The authors are grateful to the International Institute of Earthquake Engineering and Seismology (IIEES) for providing waveform data recorded by the broadband seismic stations. The authors also acknowledge data supports from the websites of Institute of Geophysics, University of Tehran (IGUT), International Seismological Centre (ISC), U.S. Geological Survey (USGS) and Global Centroid Moment Tensor (GCMT).

References

- Agard, P., Omrani, J., Jolivet, J., Whiterurch, H., Vrielynck, B., Spakman, W., Monie, P., Meyer, B., and Wortel, R., 2011, Zagros orogeny: a subduction-dominated process: *Geological Magazine*, **148**, 692-725.
- Allen, M., Jackson, J., and Walker, R., 2004, Late Cenozoic reorganization of the Arabia-Eurasia collision and the comparison of short-term and long-term deformation rates: *Tectonics*, **23**(2).
- Ambraseys, N. N., and Melville, C. P., 1982, *A History of Persian Earthquakes*: Cambridge University Press.
- Berberian, M., 2014, *Earthquakes and Coseismic Surface Faulting on the Iranian Plateau: A Historical, Social and Physical Approach*, Berberian, M., (ed.): Elsevier, *Developments in Earth Surface Processes*, **17**, 714, ISBN: 978-0-444-63292-0, First Edition.
- Bouchon, M., 1981, A simple method to calculate Green's functions for elastic layered media: *Bull. Seism. Soc. Am.*, **71**(4), 959-971.
- Bouchon, M., 2003, A review of the discrete wavenumber method: *Pure and Applied Geophysics*, **160**(3), 445-465.
- Dewey, J. F., Hempton, M. R., Kidd, W. S. F., and Saroglu, F., 1986, Shortening of continental lithosphere: the neotectonics of eastern Anatolia, a young collision zone: *Geological Society Special Publication*, **19**, 3-36.
- Hempton, M. R., 1987, Constraints on Arabian plate motion and extensional history of the Red Sea: *Tectonics*, **6**, 687-705.
- Hessami, K., Jamali, F., and Tabassi, H., 2003, Major Active Faults of Iran, Scale 1:25,000,000: *International Institute of Earthquake Engineering and Seismology*.
- Jackson, J. A., and McKenzie, D., 1984, Active tectonics of the Alpine-Himalayan belt between western Turkey and Pakistan: *Geophysical Journal of the Royal Astronomical Society*, **77**, 185-264.
- Khodaverdian, A., Zafarani, H., Rahimian, M., and Dehnamaki, V., 2016, Seismicity parameters and spatially smoothed seismicity model for Iran: *Bull. Seism. Soc. Am.*, **106**(3), 1133-1150.
- Kikuchi, M., and Kanamori, H., 1991, Inversion of complex body waves-III: *Bull. Seism. Soc. Am.*, **81**, 2335-2350.
- Lay, Th., and Wallace, T., 1995, *Modern Global Seismology*: Academic Press.
- Lienert, B. R. E., Berg, E., and Frazer, L. N., 1986, Hypocenter: An earthquake location method using centered, scaled, and adaptively least squares: *Bull. Seism. Soc. Am.*, **76**, 771-783.
- Lienert, B. R. E., and Havskov, J., 1995, A computer program for locating earthquakes both locally and globally: *Seismol. Res. Lett.*, **66**(5), 26-36.
- McKenzie, D., 1972, Active tectonics of the Mediterranean region:

- Geophysical Journal of the Royal Astronomical Society, **30**, 109-185.
- Mouthereau, F., Lacombe, O., and Verge, J., 2012, Building the Zagros collisional orogen: timing, strain distribution and the dynamics of Arabia/Eurasia plate convergence: *Tectonophysics*, **532-535**, 27-60.
- Nemati, M., Talebian, M., Sadidkhouy, A., Mirzaei, N., and Gheitanchi, M. R., 2012, Detailed crustal discontinuities, seismotectonic and seismicity parameters of the east-middle Alborz, Iran, flower structure of subsurface fault geometry: *Journal of the Earth and Space Physics*, **38**(2), 1-15.
- Nissen, E., Tatar, M., Jackson, J. A., and Allen, M. B., 2011, New views on earthquake faulting in the Zagros fold-and-thrust belt of Iran: *Geophys. J. Int.*, **186**(3), 928-944.
- Norouzi, N., and Hashemi S. N., 2016, Assessing and characterizing of seismogenic zones in Iran using GIS-based spatial analysis techniques: *International Geoinformatics Research and Development Journal*, **7**(3).
- Shearer, P. M., 2009, *Introduction to Seismology*: Cambridge University Press.
- Sokos, E. N., and Zahradnik, J., 2008, ISOLA A Fortran code and a Matlab GUI to perform multiple-point source inversion of seismic data: *Computers & Geosciences*, **34**(8), 967-977.
- Sokos, E., and Zahradnik, J., 2009, A Matlab GUI for use with ISOLA Fortran codes, User's Guide.
- Sokos, E., and Zahradnik, J., 2013, Evaluating centroid-moment-tensor uncertainty in the new version of ISOLA software: *Seismol. Res. Lett.*, **84**(4), 656-665.
- Talebian, M., and Jackson, J., 2004, A reappraisal of earthquake focal mechanisms and active shortening in the Zagros mountains of Iran: *Geophysical Journal International*, **156**(3), 506-526.
- Vackar, J., Burjanek, J., Gallovic, F., Zahradnik, J., and Clinton, J., 2017, Bayesian ISOLA: new tool for automated centroid moment tensor inversion: *Geophysical Journal International*, **210**, 693-705.
- Zahradnik, J., and Custodio, S., 2012, Moment tensor resolvability: Application to southwest Iberia: *Bull. Seism. Soc. Am.*, **102**(3), 1235-1254.
- Zahradnik, J., Gallovic, F., Sokos, E., Serpetsidaki, A., and Tselentis, A., 2008, Quick fault-plane identification by a geometrical method: Application to the Mw 6.2 Leonidio earthquake, 6 January 2008, Greece: *Seismol. Res. Lett.*, **79**(5), 653-662.
- Zahradnik, J., Sokos, E., Tselentis, G. A., and Martakis, N., 2008, Non-double-couple mechanism of moderate earthquakes near Zakynthos, Greece, April 2006; explanation in terms of complexity: *Geophysical Prospecting*, **56**(3), 341-356.